Desalination and Water Treatment
www.deswater.com

doi: 10.5004/dwt.2023.29898

307 (2023) 202–211
September

Efficient removal of neutral red dye using microporous materials: synthesis, isotherms, and kinetics studies

Affaf Tabti[a,*], Abderazzak Baba Ahmed[a], Fathi Boudahri[b]

[a]*Faculty of Science and Technology, Relizane University, 48000 Relizane, Algeria, Tel.: 00213773818688; email: affaf.affaf@yahoo.fr (A. Tabti), Tel.: 00213697896619; email: abderrazak_baba@yahoo.fr (A.B. Ahmed)*
[b]*Faculty of Technology, Department of Electrical Engineering, Abou Bekr Belkaid University, 13000 Tlemcen, Algeria, Tel.: 00213541625345; email: fethiboudahri@yahoo.com*

Received 26 March 2023; Accepted 22 August 2023

ABSTRACT

The objective of this study was to determine the power of four microporous materials synthesized not incorporated (S-1, ZSM-5) and incorporated into metals (VS-1, CuZSM-5) in the degradation of a cationic dye (Neutral Red). These materials were synthesized in a fluorinated medium under well-defined temperature and crystallization time conditions. They were characterized by different techniques, X-ray diffraction (XRD), infrared spectroscopy (IR), and ultraviolet-visible spectroscopy (UV-Vis). The degradation of the neutral red (NR) dye on the four adsorbents was analyzed using two kinetic models to study the adsorption process: pseudo-first-order and pseudo-second-order. Parameters affecting the dye adsorption, such as pH and contact time also were studied. The adsorption kinetics were better described by the pseudo-first-order model. Isothermal models were also applied in this study, Langmuir, Freundlich, and Temkin. The adsorption of NR dye on Cu/ZSM-5 seemed to conform to the Langmuir model with a high correlation coefficient R^2 value of 0.999 and the highest adsorption capacity of 16.129 mg/g was achieved at a pH level of 5.19 and a removal rate of 98.75% could be achieved within 50 min.

Keywords: Zeolites; Silicalite-1; Cu/ZSM-5; VS-1; Degradation; Neutral red

1. Introduction

Pollution is one of the consequences of the development of technology and is a threat to the environment. The demand for industrial water has resulted in the generation of a significant amount of wastewater-containing pollutants. Notably, dyes are an important class of industrial pollutants [1,2], which greatly threatens human health and can be toxic and carcinogenic [3,4] because of the aromatic molecular structures that can make them stable and difficult to biodegrade [5].

The direct release of dyes into natural water sources results in damage to the ecosystem [6], increases water opacity, reduces sunlight transmission, and affects the photosynthesis of aquatic plants and life in the water [7].

Therefore, there are three treatment methods to remove the dyes before discharging them into the water sources: biological methods, which can degrade dyes in the presence of bacteria [8], fungi [9], yeasts [10]; a chemical method using coagulation–flocculation [11], ozonation [12] to remove the dye and physical method such as adsorption which serves to degrade dye [13].

Neutral red (RN) (or toluene red or a basic red V) is a toxic compound widely used in biological research, microbiology, and virus studies, as a general histology dye, and as a vital stain. The toxicity of this organic compound is

* Corresponding author.

due to the resulting products after its decomposition which are dangerous, such as carbon monoxide, carbon dioxide, hydrogen chlorides, and nitrogen oxides [14].

Adsorption is considered a very effective method for dye removal. Researchers are conducting studies on the feasibility of using low-cost materials with large pores such as zeolites and MCM-41[15]. Harpreet et al. studied the adsorption of neutral red (NR) in the presence of Cd-M OF as an adsorbent [16], and Zhou et al. carried out the degradation of the same dye (NR) on a polymer [17]. Brião et al. [18] used a mesoporous zeolite (ZSM-5) synthesized in the adsorption of Crystal Violet dye. The activated carbon biosorbents from the *Lantana camara* were used as adsorbents for the removal of the acidic dye tartrazine from aqueous solutions [19]. Nanocomposite has also been applied for the decolorization of toxic food dyes (rhodamine B and tartrazine) from wastewater [20]. Ani et al. [21] carried out a study of the adsorption of the Red Congo using a zeolite synthesized (ZSM-5) directly from Bangka kaolin without an organic template, hierarchical zeolite-based biomembrane [22] and ZSM-5 zeolite synthesized from the biomass power plant as an adsorbent [23]. Ali et al. [24] studied the degradation of the same dye using a commercial zeolite as an adsorbent. Seyed et al. [25] performed an adsorption study of Orange Acridine on an incorporated zeolite (Fe/ZSM-5). An elimination study of Methylene Blue (MB) was carried out in the presence of a synthesized zeolite from coal fly by Dwiredi [26], and titanium silicalite-1 (TS-1) was used in the degradation of the same dye by Sean [27]. These zeolites are crystalline aluminosilicates with molecular-sieving properties. They belong to a group of tectosilicates. Each zeolite has its own distinctive crystalline and porous structures. Mesoporous Silicalite-1, ZSM-5 zeolite, and high silica zeolite are used for the adsorption of Methylene Blue [28–30]. Bouchra et al. [31] performed a Basic Fuchsin (BF) dye removal study using synthesized Fe-ZSM-5 as an adsorbent.

In this study, microporous zeolite materials (silicalite-1, vanadium-incorporated silicalite-1, ZSM-5 zeolite, and copper-incorporated zeolite) were synthesized using the hydrothermal method and used for the removal of neutral red dye. Analysis such as XRD, UV-vis, and IR spectroscopy confirmed that our materials were well crystallized and corresponded to MFI-type zeolite. The effects of contact time and solution pH on the adsorption behavior of NR were investigated. The adsorption kinetics and isotherm models that describe the elimination of the neutral red dye in the presence of S-1, VS-1, ZSM-5, and Cu/ZSM-5 as adsorbents have been presented in this work. The adsorption process of the neutral red dye in the presence of Cu/ZSM-5 as an adsorbent was best described by a pseudo-second-order kinetic model and the Langmuir isotherm, while the dye removal using S-1 and VS-1 as an adsorbent was explained by the pseudo-first-order kinetic model and two isotherms (Freundlich and Temkin).

2. Experimental set-up

2.1. Synthesis of materials

We are mainly interested in the synthesis of zeolite materials type MFI. We chose material (S-1) as the reference sample to describe the synthesis procedure of each material [32].

Silicalite-1 is synthesized from a gel containing reagents, Ludox, tetrapropylammonium hydroxide (TPAOH), Potassium fluoride (KF), and water. In a beaker, 7.5 g of Ludox is introduced into 13.50 g of water, successively adding 3.25 g of TPAOH and 2.90 g of KF. This mixture is stirred for 2 h at room temperature until a homogeneous mixture has been obtained. Then the resulting gel with a molar composition: KF-0.08TPAOH-SiO_2-20H_2O was transferred to a Teflon-coated autoclave and heated under static conditions at 175°C for 24 h. Then the autoclave was cooled. The recovered mixture was then filtered and washed several times with distilled water. The resulting product was then dried. Finally, the sample was calcined at 550°C for 6 h. (The same procedure was applied for samples MS-1, ZSM-5, and MZSM-5, adding the metal source for the incorporated materials).

2.2. Characterization of samples

The prepared materials were characterized by the X-ray diffraction patterns of the same material between 10° and 50° using a Bruker AXS D8 Advance diffractometer with a graphite monochromator using the Cu K radiation (λ = 1.5418 A) and the diffuse reflectance UV-Vis. was obtained at room temperature between 200 and 800 nm on a UV-Vis Varian Cary 5E spectrometer equipped with a double monochromator and an integrating sphere coated with polytetrafluoroethylene (PTFE) has been used.

2.3. Adsorption experiments

The neutral red dye degradation test is presented as follows: 250 mL of a solution of the neutral red with a concentration of 10 mg/L is introduced into a beaker of 250 mL afterward also adding the prepared materials (0.5 mg of S-1, ZSM-5, MS-1, and MZSM-5); this mixture is stirred for 60 min at room temperature (25°C). By measuring the pH of the solution every 10 min it was filtered using a centrifuge-type EBA-Hetlich at a speed of 3500 rpm for 15 min. Absorbance is measured at 660 nm using an OPTIZEN spectrophotometer.

A 10 mg/L concentration solution prepared by dilution from a stock solution of RN dye 1 g/L, was chosen to determine the maximum wavelength (λ_{max}) of the dye. The extrapolation of the results obtained gives us band absorption at 520 nm, which is λ_{max} for which the absorbance is maximal.

The absorbance of a neutral red solution was measured when the pH of the solution changed, an evolution in the UV-Vis spectrum (variation of λ_{max}), and an evolution in the color of the NR solution was observed. In our case, the solution prepared with 10 mg/L of the NR dye had a visible band located at a λ_{max} of 520 nm.

3. Adsorption kinetics and isotherms

3.1. Study of the adsorption kinetics

Kinetics models were considered to analyze the obtained experimental results. Two models were studied

to describe the adsorption of our dye on the four adsorbents used: the pseudo-first-order model Eq. (2) and the pseudo-second-order model Eq. (3) [33]. The kinetics of adsorption of the dye studied (NR) were carried out for an initial dye concentration of 10 mg/L, with a concentration of 0.50 g/L for the four types of adsorbent (S-1, ZSM-5) and (MS-1, MZSM-5).

The adsorption efficiency of the dye on the four adsorbents is defined by [34]:

$$R\% = \frac{\left(C_0 - C_t\right)}{C_0} \times 100 \quad (1)$$

where C_0: initial concentration of substrate (mg/L); C_t: the substrate concentration at the equilibrium of the adsorption process (mg/L).

The pseudo-first-order kinetic equation is represented by the following linear relation:

$$\log\left(q_e - q_t\right) = \log q_e - \frac{k_1 \times t}{2.303} \quad (2)$$

where q_t (mg/g) and q_e (mg/g) are the adsorption capacities at a given time t (min) and the equilibrium condition, respectively, and k_1 (min^{-1}) is the pseudo-first-order constant.
The second model is represented by the following equation:

$$\frac{t}{q_t} = \frac{1}{k_2 \times q_e^2} + \frac{t}{q_e} \quad (3)$$

where q_t is the quantity of dye adsorbed at time t (mg/g), q_e is the maximum adsorption capacity of the pseudo-second-order (mg/g), and k_2 is the kinetic constant of adsorption of the pseudo-second-order (g/mg·min).

3.2. Adsorption isotherms

Adsorption isotherms play an important role in determining the maximum adsorption capacities and in the design of new adsorbents. There are many theoretical models for describing the adsorption isotherms. In our study, we were only interested in the Langmuir equation (Eq. (4) [35], Freundlich Eq. (5) [36], and Temkin Eq. (6) [37] models. These models are given by the following equations:

$$\frac{C_e}{q_e} = \frac{1}{q_{\max} \times K_L} + \frac{1}{q_{\max} \times C_e} \quad (4)$$

$$\ln q_e = \ln K_F + \frac{1}{n} \ln C_e \quad (5)$$

$$q_e = b \ln K_T + b \ln C_e \quad (6)$$

where K_L is the Langmuir adsorption equilibrium, the constant $q_{\max}$ (mg/g) represents the maximum adsorption capacity, K_F is the Freundlich constant (L/kg), $1/n$ is the heterogeneity factor, b is the variation of adsorption energy (J/mol), and K_T is Temkin constant (L/mg).

4. Results and discussion

4.1. Characterization

4.1.1. X-ray diffraction

The diffractograms presented in Fig. 1a–e shows a well-crystallized framework and indicate the absence of an amorphous phase in the synthesized materials. The samples (E_1, E_2, E_3, and E_4), which represent S-1, ZSM-5, VS-1, and CuZSM-5, respectively, have characteristic diffraction peaks at 2θ = 23.1°, 23.98°, 24.4°, 24.56°, 25.95°, 29.41°, and 29.95°, which are exclusively indexed to the structure of the MFI topology [38,39].

The peaks appearing at 2θ = 35.5° and 38.7° in the diffractogram of sample E_4 indicate the incorporation of copper (Cu) atoms into ZSM-5[40], and the peak observed at 2θ = 23° in the E_3 sample diffractogram usually indicates orthorhombic symmetry [41].

4.1.2. UV-Vis spectroscopy

This technique is used to obtain information on the coordination environment and the oxidation states of metal ions. The UV-Vis spectra of VS-1 and Cu/ZSM-5 are shown in Fig. 2a and b.

The VS-1 spectra were dominated by four characteristic bands of charge transfer (CT) from oxygen to metal. According to the literature, the CT band centered at approximately 230–240 nm has been attributed to the tetrahedral structure of $(SiO)_3V^V$ = O located in the silica framework [42,43].

In the case of Cu/ZSM-5, we have absorption bands at 208, 265, and 348 nm, which are associated with the tetrahedral coordination environment in the transition state of charge transfer, confirming the presence of our metal inside the ZSM-5, and the bands around 265 and 348 nm correspond to the identification of extra-structures that can be attributed to the copper oxides clusters and nanoparticles of copper oxides [44].

4.2. Adsorption study

4.2.1. Effect of pH

The initial pH of the solution was a necessary factor for dye degradation. In this work, the pH of Neutral Red eliminated on the four adsorbents varied as follows:

The range of the variation of our factor is between 7.80 and 8.94, 7.19 and 8.63 when we used silicalite-1 (S-1) and zeolite (ZSM-5) as adsorbents, respectively. In the case of silicalite-1 incorporated on vanadium (VS-1) and the zeolite incorporated on copper (Cu/ZSM-5), the variation in our parameter is between 5.02 and 6.40, 5.19 and 5.33, respectively.

Thus, a decrease of the pH from 8.63 to 8.23 in the case of the adsorption of NR on the ZSM-5 resulted in a low dye removal rate from 1.25% to 8.75%. This is due to the strong electrostatic repulsion between the cationic dye and adsorbent.

In the dye elimination reaction on VS-1, S-1, and Cu/ZSM-5, the decrease in pH was from 6.40 to 5.13, 8.53 to 7.80, and 5.33 to 5.19 caused an increase in NR dye adsorption rate

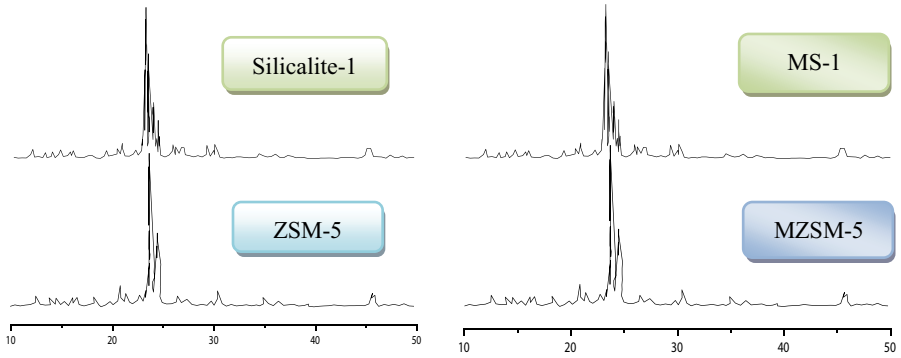

Fig. 1. Diffractograms of S-1, ZSM-5, MS-1, and MZSM-5 adsorbants.

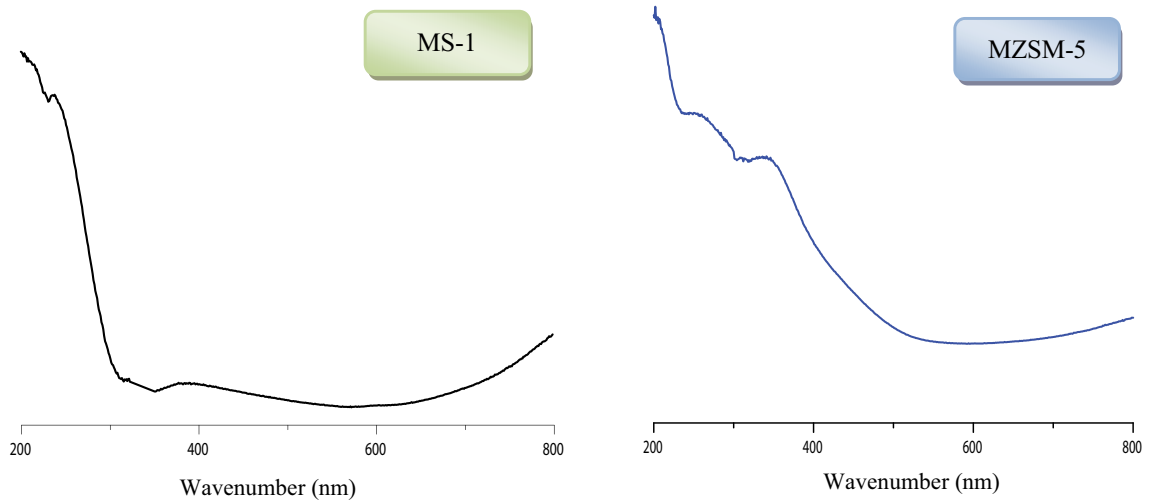

Fig. 2. UV spectra vis, (a) VS-1 and (b) Cu/ZSM-5.

from 11.25% to 45%, 22.50% to 62.50% and 82.5% to 98.75%, respectively. These results indicate the presence of an electrostatic attraction between the cationic dye and the adsorbents, which leads to an increase in the adsorption capacity of the dye.

The influence of pH on Neutral Red (NR) adsorption shows a maximum removal of dye (98.75%) at pH = 5.30, in the presence of MZSM-5 as adsorbent, and the minimum removal (8.75%) at pH = 8.54 in the presence of ZSM-5.

Fig. 3a–d show the effect of pH on pollutant degradation in the presence of adsorbents S-1, MS-1, ZSM-5, and MZSM-5.

4.2.2. Effect of contact time

The adsorption of NR was fast when we used MZSM-5 as an adsorbent, which was observed in the first 10 min with an elimination rate of 82.5%; in the presence of S-1 and MS-1, the rate of adsorption was weak in the first 10 min (22.5% and 11.25%, respectively), and the rate of elimination of NR increased with increasing time. Fig. 4 shows the adsorption capacity of NR for the adsorbents.

With ZSM-5, the adsorption rate is 1.25% in the first 10 min, indicating that there was no early interaction between the adsorbate and the adsorbent.

4.2.3. Adsorption kinetics

Concerning the pseudo-first-order, the plot of $\ln(q_e - q_t)$ as a function of time for the dye studied gives a linear form in Fig. 5, and for the pseudo-second-order, it was examined by plotting t/q_t as a function of time in Fig. 6.

All the kinetic parameters determined from these lines are collated in Table 1 on the adsorbents S-1, ZSM-5, MS-1, and MZSM-5, respectively.

From the results obtained, we notice that the first-order pseudo model is the more reliable for determining the order of the adsorption kinetics of NR on the S-1 and MS-1, and the second-order pseudo is suitable to describe the adsorption process on the ZSM-5 and MZSM-5 adsorbents because the correlation coefficients are closer to a one ($R^2 > 0.99$).

4.2.4. Adsorption isotherms

The experimental results of the NR adsorption isotherms on zeolites modeled by the Langmuir, Freundlich, and Temkin equations are shown in Figs. 7–9.

The Langmuir, Freundlich, and Temkin parameters for the NR on the four adsorbents are collated in Table 2.

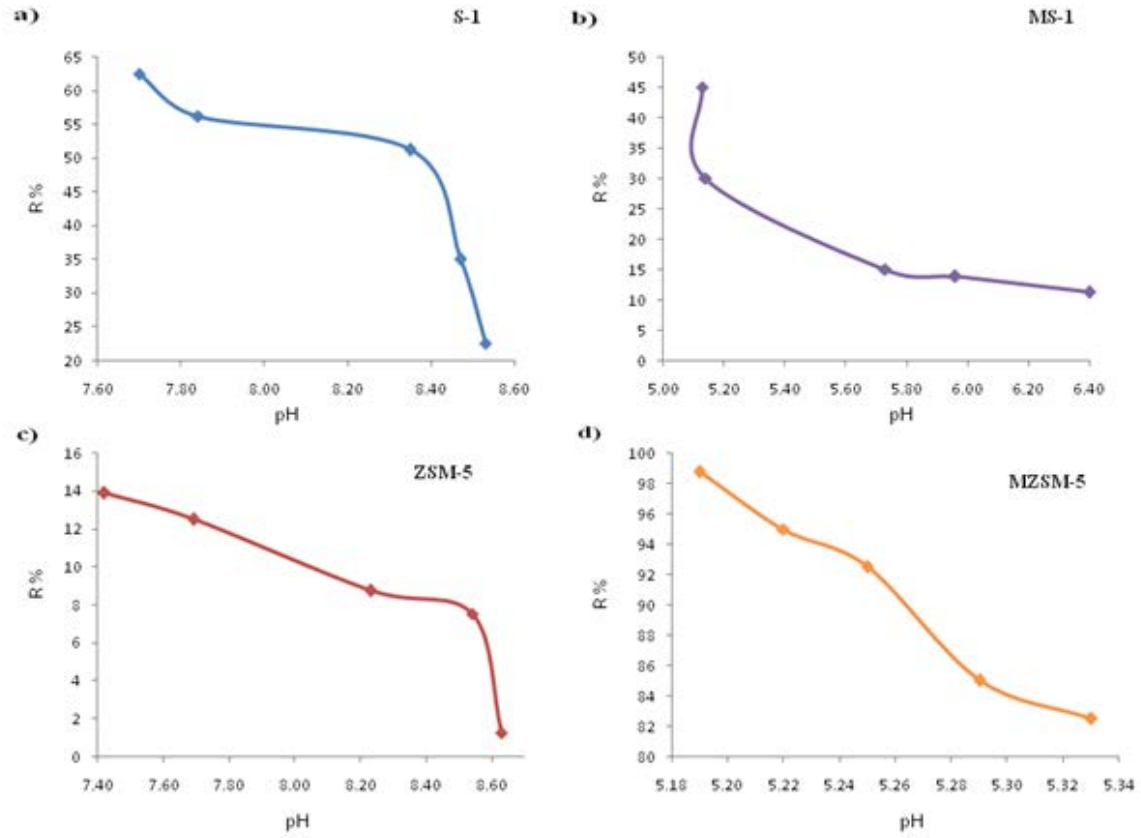

Fig. 3. Effect of pH on the adsorption of neutral red.

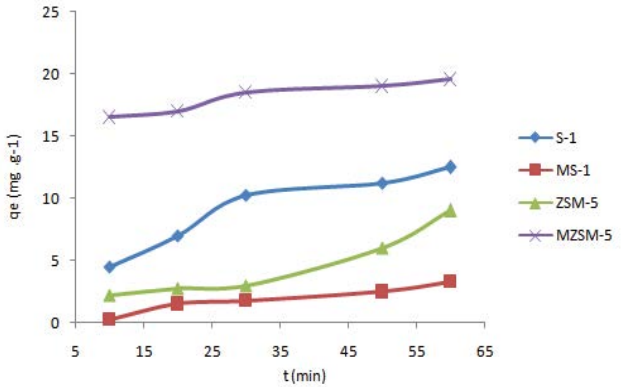

Fig. 4. Effect of contact time on the adsorption of neutral red.

We note that the correlation coefficient R^2 of the Langmuir model is very close to one for the dye on the four adsorbents. According to the constants q_{max} calculated from this model, it is observed that the adsorption capacity of NR on (MZSM-5) (q_{max} = 16.129 mg/g) is higher when compared with the other adsorbents (S-1, ZSM-5, and MS-1) (2.673, 0.207 and 1.121 mg/g), respectively.

Langmuir isotherm is characterized by the separation factor or equilibrium parameter, R_L which is used to predict whether an adsorption system is "favorable" or "unfavorable". The separation factor, R_L is defined by the following equation [45]:

$$R_L = \frac{1}{1} + \left(K_L C_0\right) \tag{7}$$

Table 1
Kinetics adsorption constants of the dye studied for the two models on the four materials (S-1, ZSM-5, VS-1, and CuZSM-5)

Dye	Adsorbents		Pseudo-first-order			Pseudo-second-order		
		q_e (Ex)	q_e (Cal)	k_1	R^2	q_e (Cal)	k_2	R^2
NR	S-1	12.5	11.34	0.46	0.987	18.510	1.881×10^{-3}	0.975
	ZSM-5	1.75	1.623	0.031	0.974	1.739	7.202×10^{-3}	0.999
	VS-1	9	7.15	0.005	0.990	37.03	1.807×10^{-4}	0.852
	CuZSM-5	19.57	5.37	0.056	0.997	20.408	1.984×10^{-2}	0.999

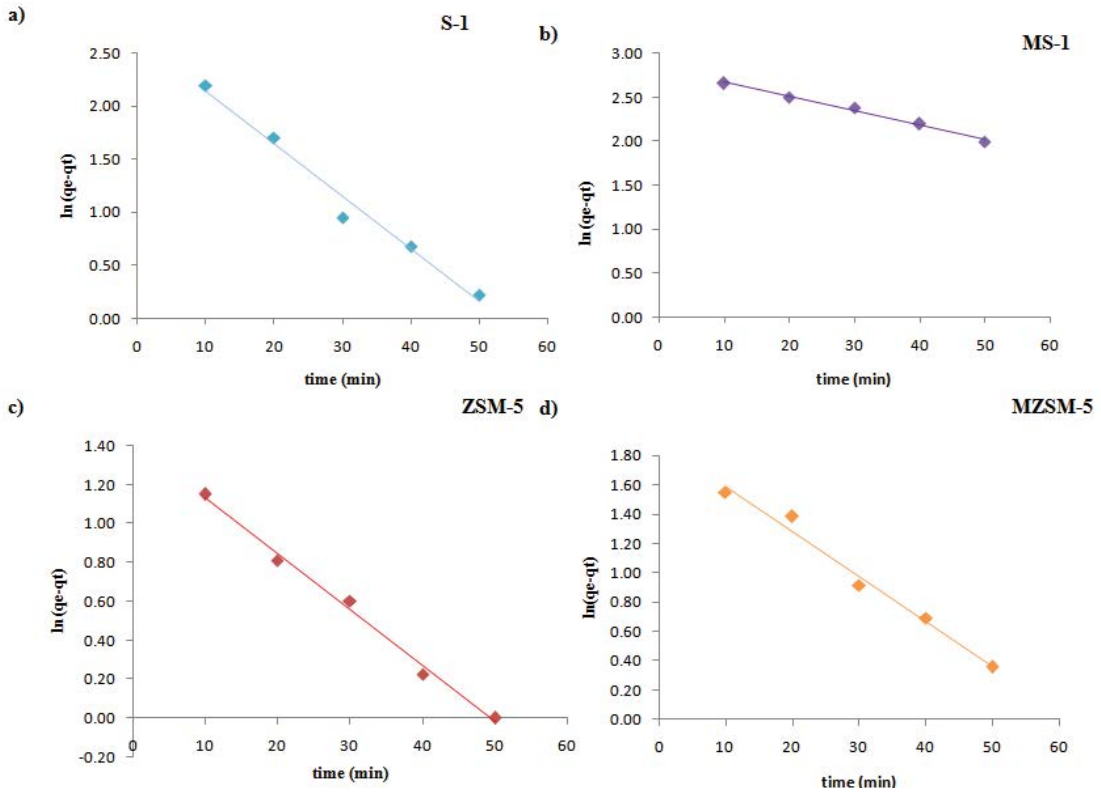

Fig. 5. Pseudo-first kinetics of neutral red for four adsorbents.

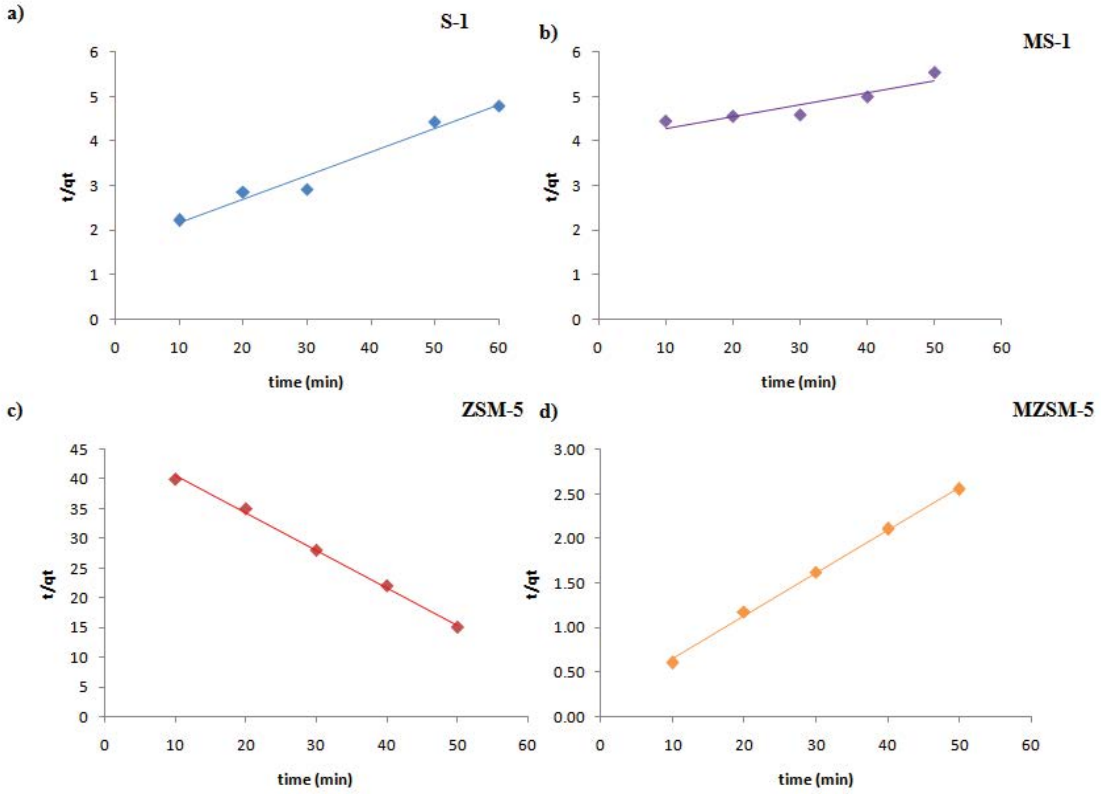

Fig. 6. Pseudo-second kinetics of neutral red for the four adsorbents.

Table 2
Adsorption isotherms constant of the dye studied on the four adsorbents (S-1, ZSM-5, VS-1, and CuZSM-5)

Langmuir				
Adsorbents	K_L	q_{max} (mg/g)	R^2	R_L
S-1	3.066×10^{-1}	2.673	0.976	2.459×10^{-1}
ZSM-5	1.25×10^{-1}	0.207	0.996	4.444×10^{-1}
CuZSM-5	2.066×10^{-1}	16.129	0.999	3.276×10^{-1}
VS-1	2.052×10^{-1}	1.121	0.947	3.276×10^{-1}
Freundlich				
Adsorbents	K_F	$1/n$	R^2	
S-1	95.106	1.469	0.968	
ZSM-5	2.653×10^{17}	40.12	0.937	
CuZSM-5	17.999	0.067	0.885	
VS-1	1.177×10^{3}	2.857	0.998	
Temkin				
Adsorbents	b (kJ/mol)	K_T	R^2	
S-1	–11.27	8.539×10^{-2}	0.992	
ZSM-5	0.465	3.061×10	0.872	
CuZSM-5	–1.137	2.014×10^{-7}	0.870	
VS-1	–13.51	9.333×10^{-2}	0.994	

The R_L values of the dye studied on the four adsorbents are in the range of $0 < R_L < 1$, which are shown in Table 2 indicating the adsorption is favorable.

In the case of the Freundlich isotherm, the results obtained show that the correlation coefficients R^2 are good in all cases. According to the values $1/n$ found, we can say that we have better adsorption of our dye on (MZSM-5), easy adsorption of the dye on (S-1 and MS-1), and difficult adsorption in the presence of ZSM-5. So, the adsorption is favorable in the presence of (MZSM-5, S-1 and MS-1) [46–48].

Concerning the Temkin isotherm, we also notice that the values of the correlation coefficient R^2 are also high for S-1 and MS-1, compared with the other two adsorbents, so the process of adsorption of NR is better with this model in the presence of S-1 and VS-1 as adsorbents. The isothermal model of Temkin thus suggests the heterogeneity of the adsorption sites of the zeolite particles [49]. The value of R^2 is lowered when the Cu/ZSM-5 was used as adsorbent. This result shows the unfavorability of the Temkin model for the studied adsorption system with this material [50].

5. Conclusion

In this research, we can say that the study of adsorption of the basic dye (NR) on four adsorbents shows that the zeolite incorporated into the metal (Cu/ZSM-5) is very suitable for the elimination of our dye, the amount of adsorbed dye is increased by increasing the contact time.

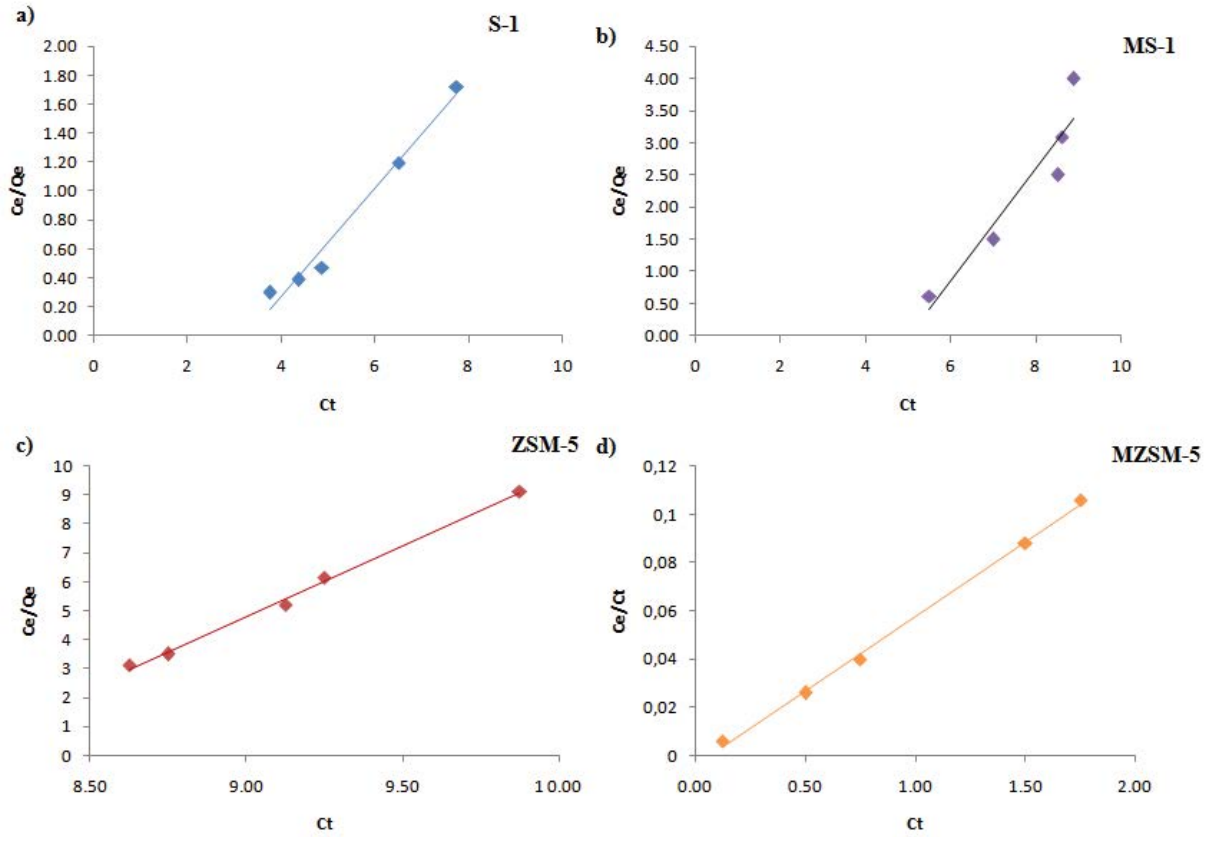

Fig. 7. Langmuir adsorption isotherm of NR on the four adsorbents.

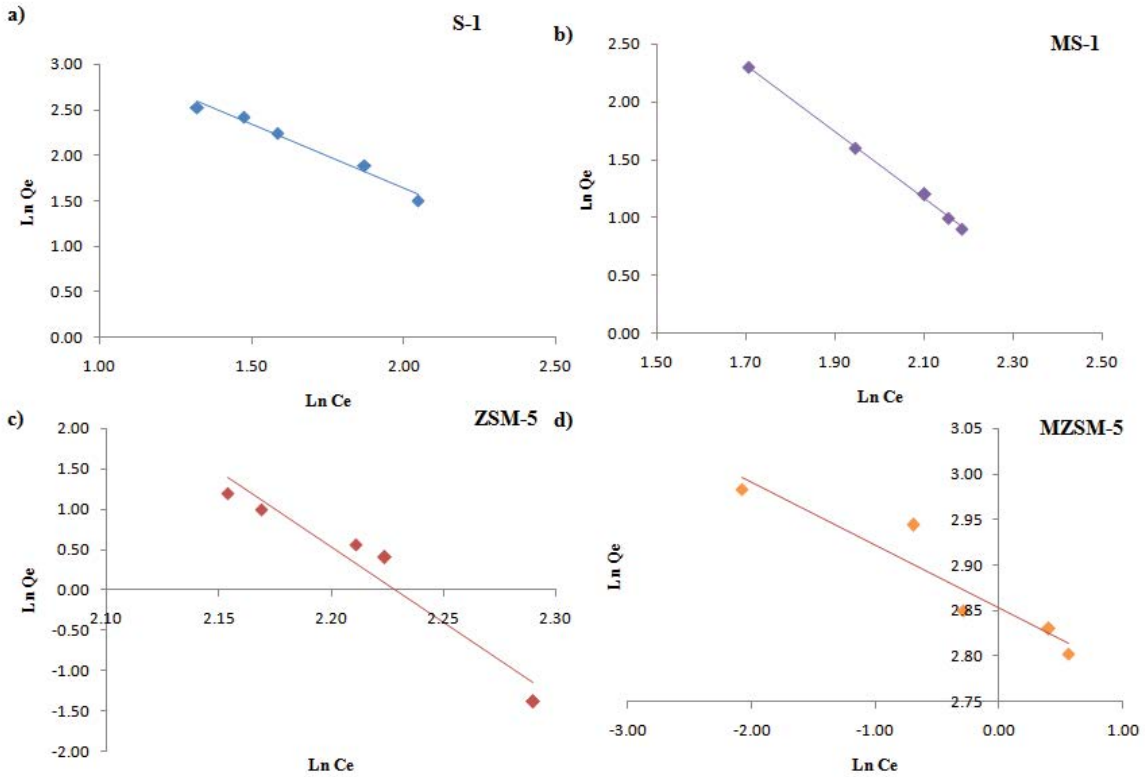

Fig. 8. Freundlich adsorption isotherm of neutral red on the four adsorbents.

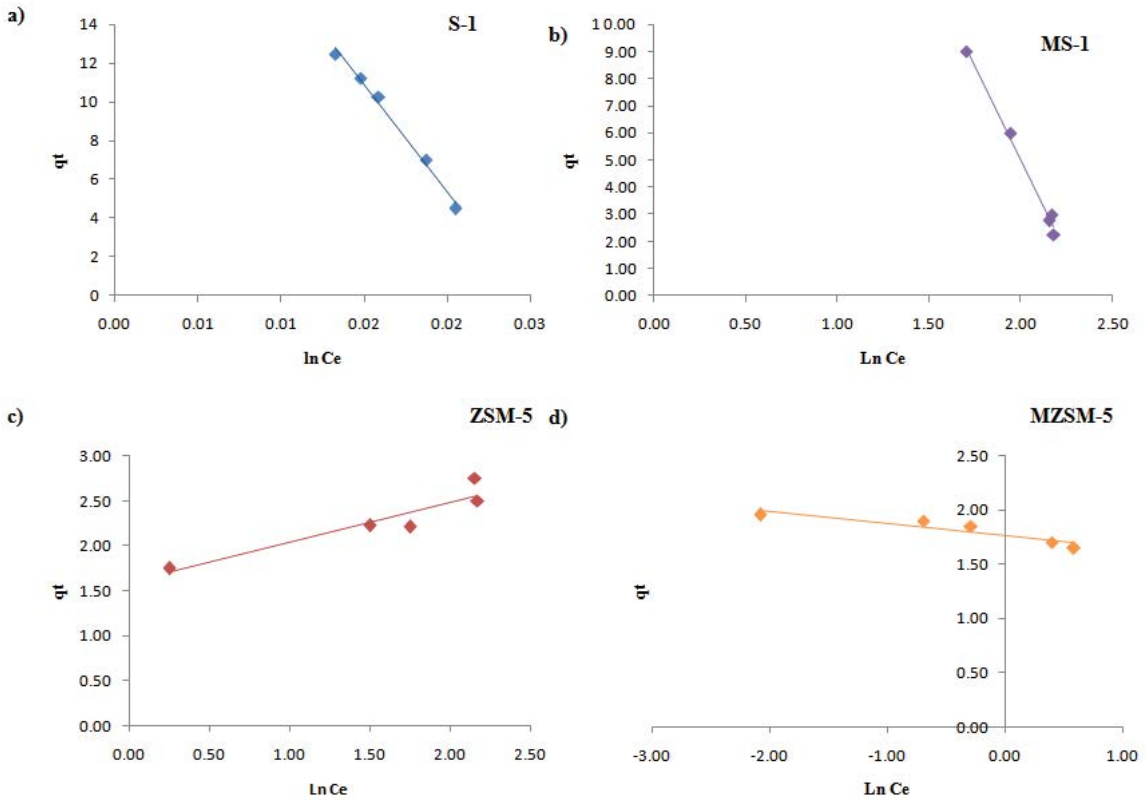

Fig. 9. Temkin adsorption isotherm of NR on the four adsorbents.

According to the results obtained, the elimination of our dye on Cu/ZSM-5 in the acidic medium is maximal with a high percentage of degradation (98.75%), we can say that we have almost total elimination at recorded time 50 min. The degradation of NR on a zeolite purely silicic (S-1) gave us a degradation rate exceeding 50% (62.50%) in a basic medium at a given moment of 50 min. The use of the vanadium-incorporated silicalite-1 in this degradation gave an elimination rate which less than 50% (45%) at a time of 60 min and a low neutral red dye removal in the presence (8.75%) of the non-metal-incorporated zeolite (ZSM-5) with a degradation rate is very low less than 10% at a time of 30 min, beyond that there was no color change.

References

[1] Z. Aksu, Biosorption of reactive dyes by dried activated sludge: equilibrium and kinetic modeling, Biochem. Eng. J., 7 (2001) 79–84.

[2] Z. Aksu, Application of biosorption for the removal of organic pollutants, a review, Process Biochem., 40 (2005) 997–1026.

[3] M. Boeninger, The Carcinogenicity and Metabolism of Azo Dyes, Especially Those Derived from Benzidine, Publication, U.S. Department of Health and Human Services, National Institute for Occupational Safety and Health, 1980, pp. 80–119.

[4] R. Anliker, Ecotoxicology of dyestuffs-a joint effort by industry, Ecotoxicol. Environ. Saf., 3 (1979) 59–74.

[5] M.W. Chang, C.C. Chung, J.M. Chern, T.S. Chen, Dye decomposition kinetics by UV/H_2O_2: initial rate analysis by effective kinetic modeling methodology, Chem. Eng. Sci., 65 (2010) 135–140.

[6] Z. Lou, R. Li, J. Liu, Q. Wang, Y. Zhang, Y. Li, Used dye adsorbent derived N-doped magnetic carbon foam with enhanced electromagnetic wave absorption performance, J. Alloys Compd., 854 (2021) 157286–157299.

[7] R.J. Ganaie, S. Rafiq, A. Sharma, Recent advances in physico-chemical methods for removal of dye from wastewater, IOP Conf. Ser.: Earth Environ. Sci., 1110 (2023) 012040–012056.

[8] M. Sudha, A. Saranya, G. Selvakumar, N. Sivakumar, Microbial degradation of azo dyes: a review, Int. J. Curr. Microbiol. Appl. Sci., 3 (2014) 670–690.

[9] Q. Yang, M. Yang, K. Pritsch, A. Yediler, A. Hagan, A. Schloter, A. Kettrup, Decolorization of synthetic dyes and production of manganese-dependent peroxidase by new fungal isolates, Biotechnol. Lett., 25 (2003) 709–713.

[10] X. Xiao, C.C. Xu, Y.M. Wu, P.J. Cai, W.W. Li, D.L. Du, H.Q. Yu, Biodecolorization of Naphthol Green B dye by *Shewanella oneidensis* MR-1 under anaerobic conditions, Bioresour. Technol., 110 (2012) 86–90.

[11] L.W. Man, P. Kumar, T.T. Teng, K.L. Wasewar, Design of experiments for Malachite Green dye removal from wastewater using thermolysis coagulation-flocculation, Desal. Water Treat., 40 (2012) 260–271.

[12] I.A. Shaikh, F. Ahmed, A.R. Sahito, A.A. Pathan, *In-situ* decolorization of residual dye effluent in textile jet dyeing machine by ozone, Pak. J. Anal. Environ. Chem., 15 (2014) 71–76.

[13] S. Dawood, T. Sen, Review on dye removal from its aqueous solution into alternative cost effective and non-conventional adsorbents, J. Chem. Process Eng., 1 (2014) 104–114.

[14] M. Irama, C. Guo, Y. Guan, A.H. Li. Ishfaq, Adsorption and magnetic removal of neutral red dye from aqueous solution using Fe_3O_4 hollow nanospheres, J. Hazard. Mater., 181 (2010) 1039–1050.

[15] A.K. Hammed, N. Dewayanto, D. Du, Ab. M.H. Rahim, M.R. Nordin, Novel modified ZSM-5 as an efficient adsorbent for methylene blue removal, J. Environ. Chem. Eng., 4 (2016) 2607–2616.

[16] K. Harpreet, K. Rakesh, K. Ajay, K. Venkata, K. Rik Rani, Trifunctional metal-organic platform for environmental remediation: structural features with peripheral hydroxyl groups facilitate adsorption, degradation and reduction processes, Dalton Trans., 48 (2019) 915–927.

[17] X. Zhou, P. Zheng, L. Wang, X. Liu, Preparation of sulfonated poly(arylene ether nitrile)-based adsorbent as a highly selective and efficient adsorbent for cationic dyes, Polymers, 11 (2019) 32–48.

[18] G.V. Brião, S.L. Jahn, E.L. Foletto, G.L. Dotto, Adsorption of crystal violet dye onto a mesoporous ZSM-5 zeolite synthesized using chitin as a template, J. Colloid Interface Sci., 508 (2017) 313–322.

[19] R.K. Gautam, P.K. Gautam, S. Banerjee, V. Rawat, S. Soni, S.K. Sharma, M.C. Chattopadhyaya, Removal of tartrazine by activated carbon biosorbents of *Lantana camara*: kinetics, equilibrium modeling, and spectroscopic analysis, J. Environ. Chem. Eng., 3 (2015) 79–88.

[20] R.K. Gautam, N. Jaiswal, A.K. Singh, I. Tiwari, Ultrasound-enhanced remediation of toxic dyes from wastewater by activated carbon-doped magnetic nanocomposites: analysis of real wastewater samples and surfactant effect, Environ. Sci. Pollut. Res. Int., 28 (2021) 36680–36694.

[21] I. Ani, I. Mualliful Moh, H. Djoko, Adsorption study of Congo red dye with ZSM-5 directly synthesized from Bangka kaolin without an organic template, Malaysian J. Fundam. Appl. Sci., 13 (2017) 832–839.

[22] S. Radoor, J. Karayil, A. Jayakumar, J. Lee, D. Nandi, J. Parameswaranpillai, B. Pant, S. Siengchin, Efficient removal of organic dye from aqueous solution using hierarchical zeolite-based biomembrane: isotherm, kinetics, thermodynamics and recycling studies, Catalysts, 12 (2022) 886–909.

[23] G. Liang, Y. Li, C. Yang, X. Hu, Q. Li, W. Zhao, Synthesis of ZSM-5 zeolites from biomass power plant ash for removal of ionic dyes from aqueous solution: equilibrium isotherm, kinetic and thermodynamic analysis, RSC Adv., 11 (2021) 22365–22375.

[24] A. Imessaoudene, S. Cheikh, A. Hadadi, N. Hamri, J.C Bollinger, A. Amrane, H. Tahraoui, A. Manseri, L. Mouni, Adsorption performance of zeolite for the removal of Congo red dye: factorial design experiments, kinetic, and equilibrium studies, Separations, 10 (2023) 57–71.

[25] D. Seyed Karim Hassani Nejad, M. Abdolraouf Samadi, G. Mehdi, Synthesis and characterization of modified ZSM-5 nanozeolite and their applications in adsorption of Acridine Orange dye from aqueous solution, J. Porous Mater., 20 (2013) 909–916.

[26] M.K. Dwivedi, I.P. Tripathi, C. Alawa, P. Shrivastava, Removal of methylene blue dye from wastewater using zeolite synthesized from coal fly ash, IOSR-J. Appl. Chem., 12 (2019) 54–61.

[27] S.P.D. Ormond, Titanium Silicalite-1 Macrostructures for Use in Photocatalytic Removal of Organic Pollutants from Aqueous Media, Manchester Metropolitan University, 2015.

[28] Y. Ji, F. Xu, W. Wei, H. Gao, K. Zhang, G. Zhang, Y. Xu, P. Zhang, Efficient and fast adsorption of methylene blue dye onto a nanosheet MFI zeolite, J. Solid State Chem., 295 (2021) 121917–121925.

[29] H. Adel Niaei, M. Rostamizadeh, F. Maasumi, M.J. Darabi, Kinetic, isotherm, and thermodynamic studies of methylene blue adsorption over metal-doped zeolite nano-adsorbent, Phys. Chem. Res., 9 (2021) 17–30.

[30] S. Radoor, J. Karayil, A. Jayakumar, J. Parameswaranpillai, S. Siengchin, Release of toxic methylene blue from water by mesoporous silicalite-1: characterization, kinetics, and isotherm studies, Appl. Water Sci., 11 (2021) 110–121.

[31] B. Ba Mohammed, A. Hsini, Y. Abdellaoui, H. Abou Oualid, M. Laabd, M. El Ouardi, A. Ait Addi, K. Yamni, N. Tijani, Fe-ZSM-5 zeolite for efficient removal of basic Fuchsin dye from aqueous solutions: synthesis, characterization, and adsorption process optimization using BBD-RSM modeling, J. Environ. Chem. Eng., 8 (2020) 104419–104429.

[32] A. Tabti, F. Djafri, F. Launay, M. Serier, I. Benchikh, Adsorption of Bromothymol Blue (BTB) dye using four zeolites as adsorbent, Kem. Ind., 7 (2021) 243–250.

[33] S. Gupta, B.V. Babu, Removal of toxic metal Cr(VI) from aqueous solutions using sawdust as adsorbent: equilibrium, kinetics and regeneration studies, Chem. Eng. J., 150 (2009) 352–365.

[34] H. Norfariha, R. Zainab, E. Salasiah, Synthesis of nanosiliceous zeolite and its functionalization with silane derivatives, Tek. J., 62 (2013) 89–93.
[35] I. Langmuir, The constitution and fundamental properties of solids and liquids part I. solids, J. Am. Chem. Soc., 38 (1916) 2221–2295.
[36] H.Y. Zhu, R. Jiang, L. Xiao, Adsorption of an anionic azo dye by chitosan/kaolin/γ-Fe_2O_3 composites, Appl. Clay Sci., 48 (2010) 522–526.
[37] A. Ansafi, M. Khemis, M.N. Pons, P.J. Leclerc, A. Yaacoubi, A. Ben Hammou, A. Nejmeddine, Electro-coagulation of reactive textile dyes and textile wastewater, Chem. Eng. Process. Process Intensif., 44 (2005) 461–470.
[38] G.N. Vayssilov, Structural and physicochemical features of titanium silicalites, Catal. Rev. Sci. Eng., 39 (1997) 209–251.
[39] H. Norfariha, R. Zainab, E. Salasiah, Synthesis of nanosiliceous zeolite and its functionalization with silane derivatives, Tek. J., 62 (2013) 89–93.
[40] W. Xu, H. Wang, X. Zhou, T. Zhu, CuO/TiO_2 catalysts for gas-phase Hg^0 catalytic oxidation, Chem. Eng. J., 243 (2014) 380–385.
[41] Ch. Baerlocher, W.M. Meier, D.H. Olson, Atlas of Zeolite Framework Types, Elsevier, Amsterdam, The Netherlands, 2001.
[42] M.M.J. Treacy, J.B. Higgins, R. Von Ballmoos, Eds., Collection of Simulated XRD Powder Patterns for Zeolites, Elsevier, New York, 1996.
[43] R. Millini, E.P. Massara, G. Perego, G. Bellussi, Framework composition of titanium silicalite-1, J. Catal., 137 (1992) 497–503.
[44] E. Yuan, K. Zhang, G.X. Lu, Z. Mo, Z. Tang, Synthesis and application of metal-containing ZSM-5 for the selective catalytic reduction of NOx with NH_3, J. Ind. Eng. Chem., 42 (2016) 142–148.
[45] M. Kumar, P.T. Bijay, K.S. Vinod, Crosslinked chitosan/polyvinyl alcohol blend beads for removal and recovery of Cd(II) from wastewater, J. Hazard. Mater., 172 (2009) 1041–1048.
[46] H. Tang, W. Zhou, L. Zhang, Adsorption isotherms and kinetics studies of malachite green on chitin hydrogels, J. Hazard. Mater., 209–210 (2012) 218–225.
[47] H.N. Tran, S.J. You, A. Hosseini-Bandegharaei, H.P. Chao, Mistakes and inconsistencies regarding adsorption of contaminants from aqueous solutions, a critical review, Water Res., 120 (2017) 88–116.
[48] H.N. Tran, S.-J. You, H.-P. Chao, Fast and efficient adsorption of methylene green 5 on activated carbon prepared from new chemical activation method, J. Environ. Manage., 188 (2017) 322–336.
[49] C.J. Pursell, H. Hartshorn, T. Ward, B.D. Chandler, F. Boccuzzi, Application of the Temkin Model to the adsorption of CO on gold, J. Phys. Chem. C, 115 (2011) 23880–23892.
[50] R.K. Gautam, I. Tiwari, Humic acid functionalized magnetic nanomaterials for remediation of dye wastewater under ultrasonication: application in real water samples, recycling, and reuse of nanosorbents, Chemosphere, 245 (2020) 125553–125597.